UNIVERSITY OF LEEDS

This is a repository copy of *Organ on chip models for the evaluation of microbubble based therapeutic delivery*.

White Rose Research Online URL for this paper:
http://eprints.whiterose.ac.uk/161787/

Version: Accepted Version

Proceedings Paper:
Bourn, M, Batchelor, DVB orcid.org/0000-0001-6489-9578, Ingram, N orcid.org/0000-0001-5274-8502 et al. (4 more authors) (2020) Organ on chip models for the evaluation of microbubble based therapeutic delivery. In: Proceedings of Microfluidics, BioMEMS, and Medical Microsystems XVIII. Microfluidics, BioMEMS, and Medical Microsystems XVIII, 01-06 Feb 2020, San Francisco, California, USA. Society of Photo-optical Instrumentation Engineers . ISBN 9781510632332

https://doi.org/10.1117/12.2551605

© (2020) COPYRIGHT Society of Photo-Optical Instrumentation Engineers (SPIE). This is an author produced version of a conference paper published in Microfluidics, BioMEMS, and Medical Microsystems. Uploaded in accordance with the publisher's self-archiving policy.

Reuse
Items deposited in White Rose Research Online are protected by copyright, with all rights reserved unless indicated otherwise. They may be downloaded and/or printed for private study, or other acts as permitted by national copyright laws. The publisher or other rights holders may allow further reproduction and re-use of the full text version. This is indicated by the licence information on the White Rose Research Online record for the item.

Takedown
If you consider content in White Rose Research Online to be in breach of UK law, please notify us by emailing eprints@whiterose.ac.uk including the URL of the record and the reason for the withdrawal request.

White Rose university consortium
Universities of Leeds, Sheffield & York

eprints@whiterose.ac.uk
https://eprints.whiterose.ac.uk/

Organ on chip models for the evaluation of microbubble based therapeutic delivery

Matthew Bourn[a,b], Damien V. B. Batchelor[a], Nicola Ingram [b], James McLaughlan[b,c], P. Louise Coletta [b], Stephen D. Evans[a], Sally A. Peyman[a,b]
[a]School of Physics and Astronomy, University of Leeds, Leeds. UK. LS2 9JT.
[b]Leeds Institute for Medical Research, School of Medicine, St James' Hospital, Leeds. UK. LS9 7TF
[c]School of Electronic and Electrical Engineering, University of Leeds, Leeds, UK. LS2 9JT.

ABSTRACT

Current in vitro cancer models used for screening potential new therapeutic agents are often 2D monolayers of cells grown on the bottom of a petri dish or culture flask. These simplistic models lack many of the important biological features of in vivo tissue growth, such as the presence of an extracellular matrix (ECM) and cell interactions associated with this in a 3D structure. The use of spheroids for drug testing has gone some way to address the limitations of 2D cultures, however spheroids are still typically handled in static environments that neglect important physical aspects of the microenvironment present in vivo, such as fluid flow and associated shear stresses. In addition, assays involving spheroids still require many manual pipetting steps in which fluid is replaced in a single fluidic operation which is labor intensive, can be damaging to spheroid structural integrity and is an action that is physiologically incorrect. Here we present a microfluidic platform for the high-throughput trapping, culture and exposure of 3D co-culture spheroids to drugs under physiologically relevant fluid flow. The device is self-supportive, allowing multiple devices to be in an incubator at once without peripheral pumps. Spheroids can be monitored in situ with microscopy and the device is designed such that spheroids can be recovered for quantitative off-chip analysis. As a first demonstration, the effectiveness of co-delivering ultrasound (US) triggered microbubbles (MBs) with doxorubicin (DOX) was evaluated. Spheroids exposed to 3 µM DOX co-delivered with MBs showed a 51% reduction is spheroid viability compared to a 25% reduction in viability of free DOX alone.

Keywords: organ-on-chip, spheroids, microbubbles, cancer

1. INTRODUCTION

Inadequate in vitro models, such as 2D monolayer cultures, are being blamed for the difficulty in translating in vitro drug screening outcomes to in vivo models, causing a failure in the drug discovery pipeline. It is thought that 2D cultures lack the biological complexity of in vivo tissues, many features of which are thought to relate to drug resistance, such as the presence of an ECM and fluid flow. 3D spheroid culture models have been developed to overcome many of these shortcomings, using aggregates of multiple cell types to form 3D tumour models in which cells grow in a more natural 3D structure and produce ECM. In addition, the in vivo structure of solid tumours is better modelled in spheroids, displaying features such as a necrotic, hypoxic core followed by layers of quiescent cells surrounded by a rapidly proliferating outer layer [1,2]. These models are more biologically accurate to in vivo tumors and have been shown to better predict the clinical effects of new drugs compared to 2D cultures [3–6] . One of the reasons for 3D spheroids being a more accurate predictor of drug outcomes in vivo is due to the presence of an ECM in co-culture models. Fibroblasts are responsible for laying down the proteins associated with the ECM, such as collagen that contribute to the mechanical 'stiffness' of tumors. This rigidity associated with the ECM can act as a physical barrier to drug penetration, preventing cells in deeper layers of the tumour being exposed to effective drug levels and resulting in treatment failure.

When MBs are exposed to US, they oscillate and certain US conditions can cause the MB to collapse, known as MB destruction. When MBs are in close proximity to a cell this oscillation and collapse can create an effect called sonoporation in which small holes are punctured in cell membranes. This phenomenon offers a promising solution to the issue of drug penetration and has been studied extensively as a method by which drugs can be delivered to cells [7–12]. The

majority of these studies however, have been conducted on 2D monolayers of cells, meaning MB effectiveness in 3D cultures is still relatively undocumented. Recent studies have begun testing MB therapies on 3D cultures, observing the effects of delivering liposomal drugs conjugated to MBs. Roovers et al have shown that MB-induced sonoporation increases delivery of liposomal drugs to the outer spheroid layers, which then act as reservoirs slowly releasing drug. This was observed to increase drug effectiveness compared to LS alone however, no overall increase in drug effectiveness was observed compared to free drug [13]. To date, MB – spheroid interactions have been performed in static conditions, neglecting the physical microenvironment of fluid flow.

Here we present a microfluidic platform for high-throughput handling of spheroids for drug screening that features constant fluid flow at physiologically relevant velocities. The devices features an array of traps for capture and culture of pre-grown spheroids that can be reversed in function for the recovery of spheroids from the device. In addition, fluid flow is generated by integrated fluid reservoirs and hydrostatic pressure so no peripheral pumps are required, facilitating high numbers of device loading into an incubator. The platform was used to investigate the effect of co-delivering DOX with MB and US to colorectal and fibroblast co-culture spheroids under flow. We show that the presence of MBs with an US trigger with free DOX increases drug penetration and decreases cell viability (51%) compared to free DOX alone (75%).

2. EXPERIMENTAL

2.1 Reagents and assays

Colorectal HCT116 tumour cells and Human Foetal Foreskin Fibroblast (HFFF2) cells were grown and maintained in DMEM 10% FBS (Thermo Fisher), 1% Glutamax (Gibco) in an incubator at 37ºC, 5% CO_2. Prior to spheroid seeding, cell media was removed, the cells washed with PBS (+Ca, +Mg Gibco) then detached with TrypLE Express (Gibco). Cell concentrations were determined using a haemocytometer after which cells were suspended in a 1:1 ratio at a concentration of 7.5 x 10^2 cells/mL. 200 µL of cell suspension was seeded into ultra-low attachment 96 well plates (Corning, Costar) and spheroids allowed to form for 5 days. DOX (100mg, Generon) was dissolved in 5 mL DMSO then further diluted in DMEM to the required concentration. DMSO concentration was kept below 0.5% to prevent any reduction in cell viability.

CellTiter-Glo 3D cell viability assay (Promega) was used as an endpoint assay to determine spheroid viability. Spheroids were retrieved off chip 48 hours after exposure by withdrawing the chamber contents from the inlet and 100 µL of the assay reagent mixed with the spheroids in an opague-walled 96 well plate. After incubation at room temperature for 30 min the luminescence was recorded on a plate reader (SpectraMax M2E, Molecular Devices) as per assay instructions.

MBs were prepared from a mixture of DPPC and DPSE-PEG2000 in a 95:5 molar ratio and a total lipid concentration of 2 mg/mL^{-1} and produced using a microfluidic microspray device to produce 10^8 MBs/mL with an average diameter between 1 -2µm.

2.2 Microchip fabrication

Devices were fabricated in polydimethylsiloxane (PDMS, Sylgard 184, Dowsil) using standard photolithography and soft lithography techniques [14,15]. Briefly, SU8-2075 photoresist was spin coated onto a 3-inch silicon wafer then baked for 90 minutes. This process was repeated giving a total resist height of approximately 350 µm. 375 nm UV laser selectively expose the photoresist and pattern the microfluidic design. PDMS was mixed in a 10:1, base: curing agent ratio, poured onto the wafer and desiccated for 40 minutes to remove any bubbles. PDMS was then cured at 80ºC for an hour. Devices were then cut, hole-punched and bonded to PDMS coated glass microscope slides using oxygen plasma. Reservoirs were fabricated from polycarbonate (Engineering & Design Plastics). Lids were fabricated from delrin (Par-group) then 0.22 µm PTFE filters (Cole-Parmer) glued on to prevent bacterial contamination of the media.

2.3 Experimental set-up and methodology

10 spheroids, with a diameter within the range 280 - 330 µm, were loaded into each inlet reservoir and allowed to flow into the device under hydrostatic pressure. The hydrodynamic force from fluid flow ensured that spheroids remained in their traps, unless subject to backflow. Once sufficient numbers of spheroids had been trapped, media from both reservoirs was removed and the therapeutic compound added to the inlet reservoir. For MB exposures, MBs were directly pipetted into the channel through the reservoir, preventing MBs from rising to the top of the reservoir. Therapeutic exposure was stopped by simply removing all compound-containing media and refilling the inlet reservoir

with fresh media. Microfluidic devices were insonated using a 2.25 MHz centre frequency un-focused transducer (V323-SM, Olympus, US). US pulse for MB destruction was controlled by a function generator (TG5011, Agilent Technologies, UK) and consisted of a duty cycle of 1 %, pulse repetition frequency of 1 kHz and total duration of 2 seconds. Transducer output was calibrated to provide a peak negative pressure of 0.81 ± 0.04 MPa when driven by a +53 dB RF power amplifier (A150, Electronics % Innovation, US). The transducer was coupled to the top of the microfluidic device via a gel pad (Aquaflex, Parker Laboratories, US). A Leica DMi8/SP8 confocal microscope system was used for fluorescence imaging of spheroids on-chip. Doxorubicin and NucRed Dead dye were excited sequentially using 488 nm OPSL and 638 nm Diode lasers, respectively. A 10x objective was used to image spheroids in 5 µm Z-stack slices.

3. RESULTS AND DISCUSSION

3.1 Device optimization.

For any drug screening assay, the number of samples and subsequent statistical analysis is hugely important. Therefore in order to trap the maximum number of spheroids, the spheroid size and microfluidic trap dimensions were optimized. Figure 1a shows a brightfield microscopy image of 7 spheroids trapped on a single device. The traps were designed similar to those be di Carlo et al. featuring a 'pocket' in which an object such as a cell sits under constant flow[16]. The subsequent filling up of the traps depends on the offset of downstream traps relative to those upstream and a balance of fluidic resistances. The device reported here was designed to trap multi-cellular spheroids rather than single cells. The diameter of the pocket width was approximately 330 µm, the width of the trap exhaust channel was 150 µm and the total depth of the device was 350 µm. The size of the spheroid is critical to the success of the device, as smaller spheroids will not be trapped while larger spheroids will not flow through the array.

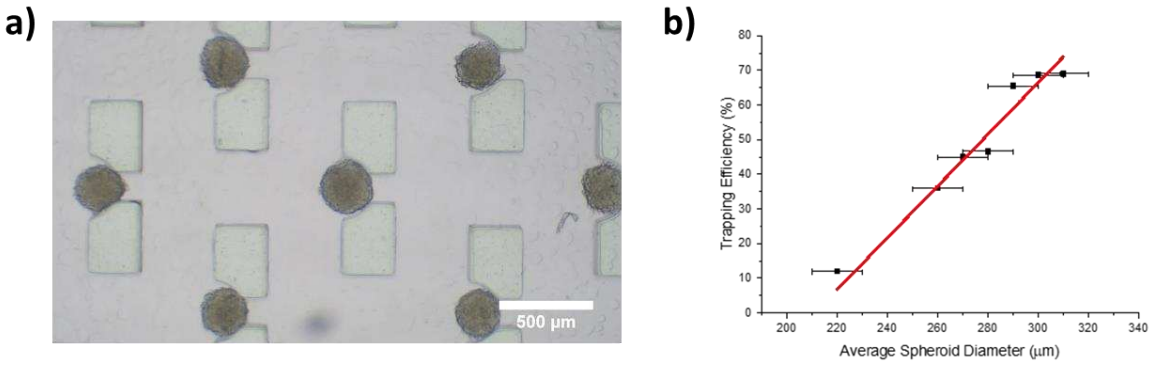

Figure 1. a) Microscopy image of spheroids (~ 300 µm) trapped in a microfluidic trap array. b) Plot of average spheroid size (220 – 320 µm) against device trapping efficiency (10 – 70%). As spheroid size increases, spheroid trapping efficiency also increases.

Figure 2b shows a plot of average spheroid size against trapping efficiency (determined by the number of available traps and those that are occupied after loading). The size of the spheroids tested were between 220 and 300 µm in diameter. The trapping efficiency is seen to increase with increasing spheroid size, with spheroids of ~300 µm having the highest trapping efficiency of 70%. Spheroids larger than 350 µm were found to stick in the channels due to the height of the device. Therefore all future experiments were performed using spheroids of approximately 300 µm in diameter.

3.2 Proof of principle DOX and MB co-delivery.

In order to demonstrate both the device as a platform for rapid drug screening against 3D co-cultures and MBs as an effective therapeutic, pre-grown spheroids of HT116 and HFFF2s were trapped and exposed to 3 µM free DOX, free DOX + US trigger and 3 µM DOX + MBs with US destruction trigger as described in the experimental section. The

concentration of 3 µM DOX was determined by producing a dose-response curve for concentrations of 0 – 10 µM with respect to spheroid viability (data not shown). The microfluidic device featured integrated reservoirs for fluid handling, in which the height difference between the inlet and the outlet provided hydrostatic pressure, which was optimized to drive flow at velocities similar to those observed in capillaries (0.3 – 1 mm/s). The devices therefore did not require any peripheral instruments such as syringe pumps and could be loaded in high numbers into a standard incubator. For the following study, spheroids were loaded onto 34 chips giving a spheroid number of n=162 and exposed to DOX for 8 h. DOX containing media was then replaced with fresh media and the spheroids allowed to grow for a further 48 h. After 48 h, NucRed stain was added to the device and washed off after 30 min to visualize cell death. Spheroids were imaged in situ using confocal fluorescence microscopy to observe DOX accumulation through its intrinsic fluorescent signal and corresponding cell death.

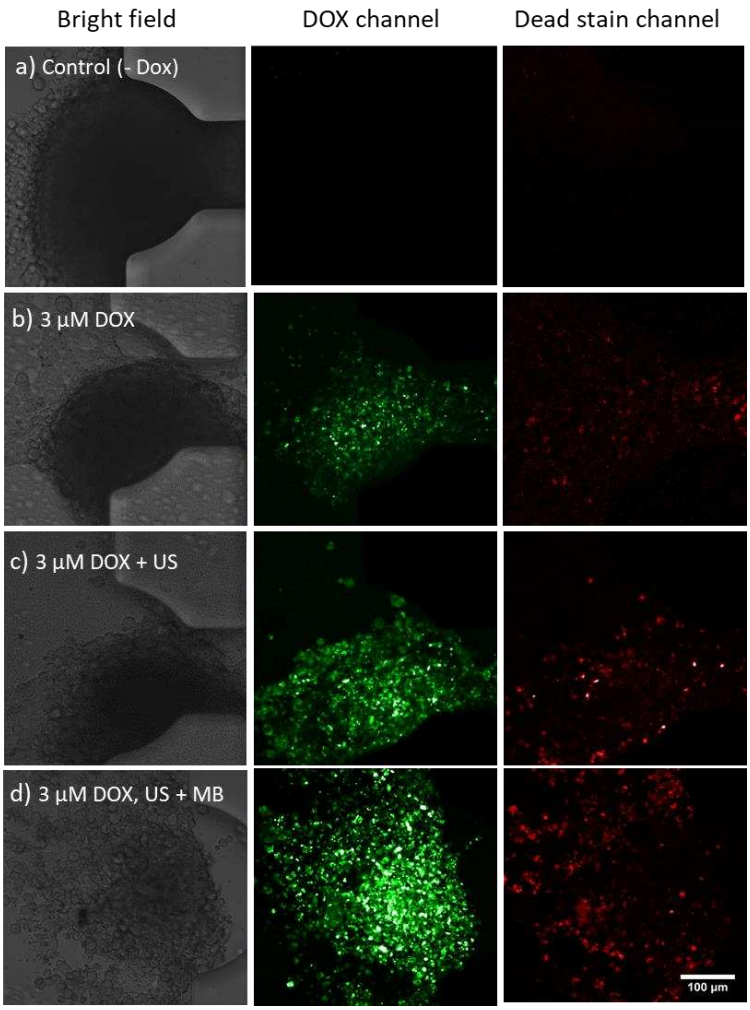

Figure 2. Bright field and confocal fluorescence images of spheroids in traps shown in bright field (first column), DOX emission (second column) and red dead stain (third column). a) Control without DOX exposure b) 3 µM free DOX c) 3 µM free DOX with US exposure and d) 3 µM DOX co-delivered with MBs and US exposure.

Figure 2 (a-d) is an image panel showing spheroids in traps imaged using bright field (first column) and fluorescence microscopy (column two and three). The bright field images show an decrease in the structural integrity of spheroids

compared to the control (a) as spheroids are exposed to 3 µM DOX (2b), 3 µM DOX with US exposure (2c) and finally, 3 µM DOX co-delivered with MBs with US exposure (2d). The loss of structural integrity through images a-d was due to the increase in the penetration of the DOX, which can be seen in the DOX channel in Figure 2 (a-d) with the inclusion of US and then MBs and US and the subsequent increase in cell death, as seen in by NucRed stain figure 2 (a-d) third column. As cells died, the cell-cell adhesion breaks down, the core density decreases and the spheroid breaks apart under flow. This effect directly correlates to the increase in DOX penetration and retention seen in column two, green signal. The presence of the US exposure increased DOX penetration into the spheroid and resulted in a slight increase in the dead stain signal compared to free DOX alone. This increase in drug penetration and subsequent cell death can be attributed to an increase in cell permeability due to the exposure to US, an effect that has been documented in the literature [17,18]. However the co-delivery of free DOX with MBs and US exposure shows the greatest loss of spheroid integrity and increase in DOX signal after 48 hours, suggesting the bursting of MBs in the vicinity of the spheroids increased drug penetration. This also correlated with increased NucRed staining, suggesting high cell death. MB destruction under US causes localized shock waves that can penetrate cell membranes, increasing the number of pores by which the drug could enter the cell.

In order to quantify cell viability in these studies, spheroids were recovered from the devices and subjected to the CellTiter-Glo 3D cell viability assay as described in the experimental section. Figure 3 shows a boxplot of cell viability (as a percentage standardized to the control), for each exposure study (free DOX, DOX + US and DOX + US + MBs).

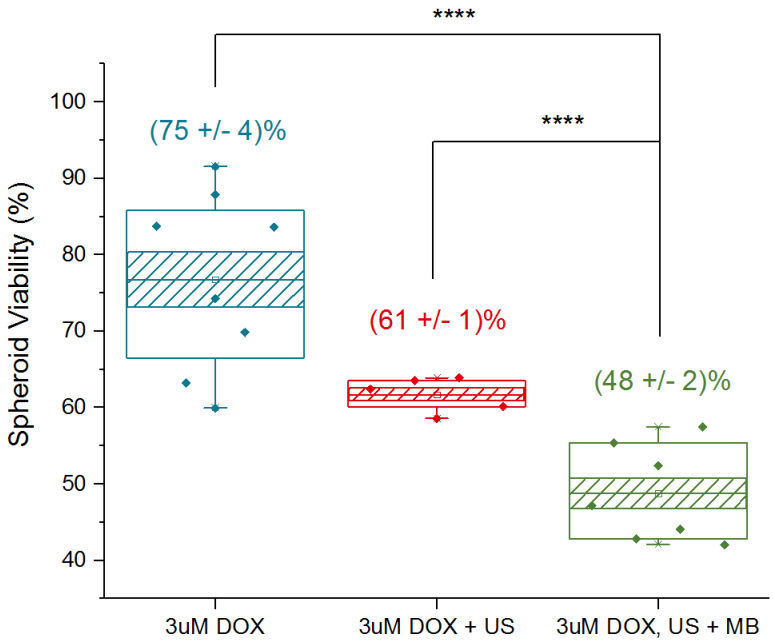

Figure 3. Boxplot showing spheroid viability in % against each exposure study, free DOX (blue), free DOX with US trigger (red) and free DOX co-delivered with US trigger (Red). Statistical significance was calculated using a Mann-Whitney (MW) non-parametric t-test with values <0.0001 (****) and 95% confidence interval (C.I.) test performed on each data set.

The cell viability for free DOX was 75 (± 4)% with a decrease with the addition of the US trigger to 61 (± 1)% and further decrease to 48 (± 2)% for co-delivery with MBs with US trigger. These results clearly show the impact of the presence of MBs and US on the penetration of DOX and subsequent cell death in CRC spheroids. The decrease in cell viability of 26% when co-delivering MBs with the US trigger compared to free DOX alone suggests the destruction of the MBs causes an increase in DOX penetration into cells, which results in an increase in cell death and thus increasing DOX efficacy. A similar spheroid viability was observed with the use of 5 µM DOX (45 (± 9) %), thus showing an increase in DOX efficacy of approximately 66% when co-delivered with MBs. These effects have been observed in previous MB studies [19–21]. The design of the microfluidic platform allowed for large numbers of spheroids (n = 161) to be analyzed under the same conditions and therefore statistical tests to be performed on the data. A MW t-test was

performed to determine their statistical significance and P-values in each case were found to be <0.0001 (****), confirming the reliability of the results. 95% C.I. calculations gave values of ± 3.6 %, ± 0.8 % and ± 2 % for DOX only, DOX + US and DOX, US + MB respectively.

4. CONCLUSIONS

We have demonstrated a microfluidic platform for the high-throughput exposure of 3D co-culture spheroids to therapeutic agents under continuous flow conditions. The device allows for the capture, culture and exposure of spheroids to drugs with minimal spheroid handling and is designed so that many devices can be used in parallel in an incubator. Devices trap spheroids with ~70% efficiency and spheroids can be recovered from the device for off-chip testing. Using this platform, we show how MBs mediated drug delivery increases the efficacy of DOX therapy in 3D CRC co-cultures under physiological flow conditions, a study that has not yet been undertaken. Free DOX co-delivered with MBs and triggered using US was shown to decrease spheroid viability by 51% compared to a decrease in viability of 25% using free DOX alone. The microfluidic device is versatile, so that spheroids of different cancer models could be used along with different potential therapeutics. Spheroids can be monitored in situ with microscopy or recovered for off-chip assessment, such as viability assays or genetic testing.

REFERENCES

1. Fennema, E., Rivron, N., Rouwkema, J., van Blitterswijk, C. & De Boer, J. Spheroid culture as a tool for creating 3D complex tissues. Trends Biotechnol. **31**, 108–115 (2013).
2. Thoma, C. R., Zimmermann, M., Agarkova, I., Kelm, J. M. & Krek, W. 3D cell culture systems modeling tumor growth determinants in cancer target discovery. Adv. Drug Deliv. Rev. **69**–**70**, 29–41 (2014).
3. Hoffmann, O. I. et al. Impact of the spheroid model complexity on drug response. J. Biotechnol. **205**, 14–23 (2015).
4. Sant, S. & Johnston, P. A. The production of 3D tumor spheroids for cancer drug discovery. Drug Discov. Today Technol. **23**, 27–36 (2017).
5. Vinci, M. et al. Advances in establishment and analysis of three-dimensional tumor spheroid-based functional assays for target validation and drug evaluation. BMC Biol. **10**, (2012).
6. Yip, D. & Cho, C. H. A multicellular 3D heterospheroid model of liver tumor and stromal cells in collagen gel for anti-cancer drug testing. Biochem. Biophys. Res. Commun. **433**, 327–332 (2013).
7. Boissenot, T., Bordat, A., Fattal, E. & Tsapis, N. Ultrasound-triggered drug delivery for cancer treatment using drug delivery systems: From theoretical considerations to practical applications. J. Control. Release **241**, 144–163 (2016).
8. Wang, M. et al. Sonoporation-induced cell membrane permeabilization and cytoskeleton disassembly at varied acoustic and microbubble-cell parameters. Sci. Rep. **8**, 1–12 (2018).
9. De Cock, I. et al. Ultrasound and microbubble mediated drug delivery: acoustic pressure as determinant for uptake via membrane pores or endocytosis. J. Control. Release **197**, 20–28 (2015).
10. Lee, H. et al. Combination of chemotherapy and photodynamic therapy for cancer treatment with sonoporation effects. J. Control. Release **283**, 190–199 (2018).
11. Lentacker, I., Geers, B., Demeester, J., De Smedt, S. C. & Sanders, N. N. Design and evaluation of doxorubicin-containing microbubbles for ultrasound-triggered doxorubicin delivery: Cytotoxicity and mechanisms involved. Mol. Ther. **18**, 101–108 (2010).
12. Kooiman, K., Vos, H. J., Versluis, M. & De Jong, N. Acoustic behavior of microbubbles and implications for drug delivery. Adv. Drug Deliv. Rev. **72**, 28–48 (2014).
13. Roovers, S. et al. Sonoprinting Liposomes on tumour spheroids by microbubbles and ultrasound. J. Control. Release 112062 (2019). doi:10.1016/j.jphotochem.2019.112062
14. Mack, C. Fundamental Principles of Optical Lithography: The Science of Microfabrication. (Wiley, 2011).
15. Kim, P. et al. Soft lithography for microfluidics: A Review. Biochip J. **2**, 1–11 (2008).
16. Carlo, D. Di, Wu, L. Y. & Lee, L. P. Dynamic single cell culture array. Lab Chip **6**, 1445–1449 (2006).
17. Yu, T., Wang, Z. & Mason, T. J. A review of research into the uses of low level ultrasound in cancer therapy. Ultrason. Sonochem. **11**, 95–103 (2004).
18. Samir Mitragotri. Healing sound the use of ultrasound in drug delivery and other therapeutic applications. Nat.

Rev. Drug Discov. **4**, 5–10 (2005).
19. Hu, Y., Wan, J. M. F. & Yu, A. C. H. Membrane Perforation and Recovery Dynamics in Microbubble-Mediated Sonoporation. Ultrasound Med. Biol. **39**, 2393–2405 (2013).
20. Nittayacharn, P. et al. Enhancing Tumor Drug Distribution With Ultrasound-Triggered Nanobubbles. J. Pharm. Sci. **108**, 3091–3098 (2019).
21. Yoshida, T. et al. Combination of doxorubicin and low-intensity ultrasound causes a synergistic enhancement in cell killing and an additive enhancement in apoptosis induction in human lymphoma U937 cells. Cancer Chemother. Pharmacol. **61**, 559–567 (2008).